

Supporting Information

Intermolecular Vibrational Energy Transfers in Liquids and Solids

Hailong Chen, Xiewen Wen, Xunmin Guo, Junrong Zheng*

Department of Chemistry, Rice University, Houston, TX

*To whom correspondence should be addressed: junrong@rice.edu

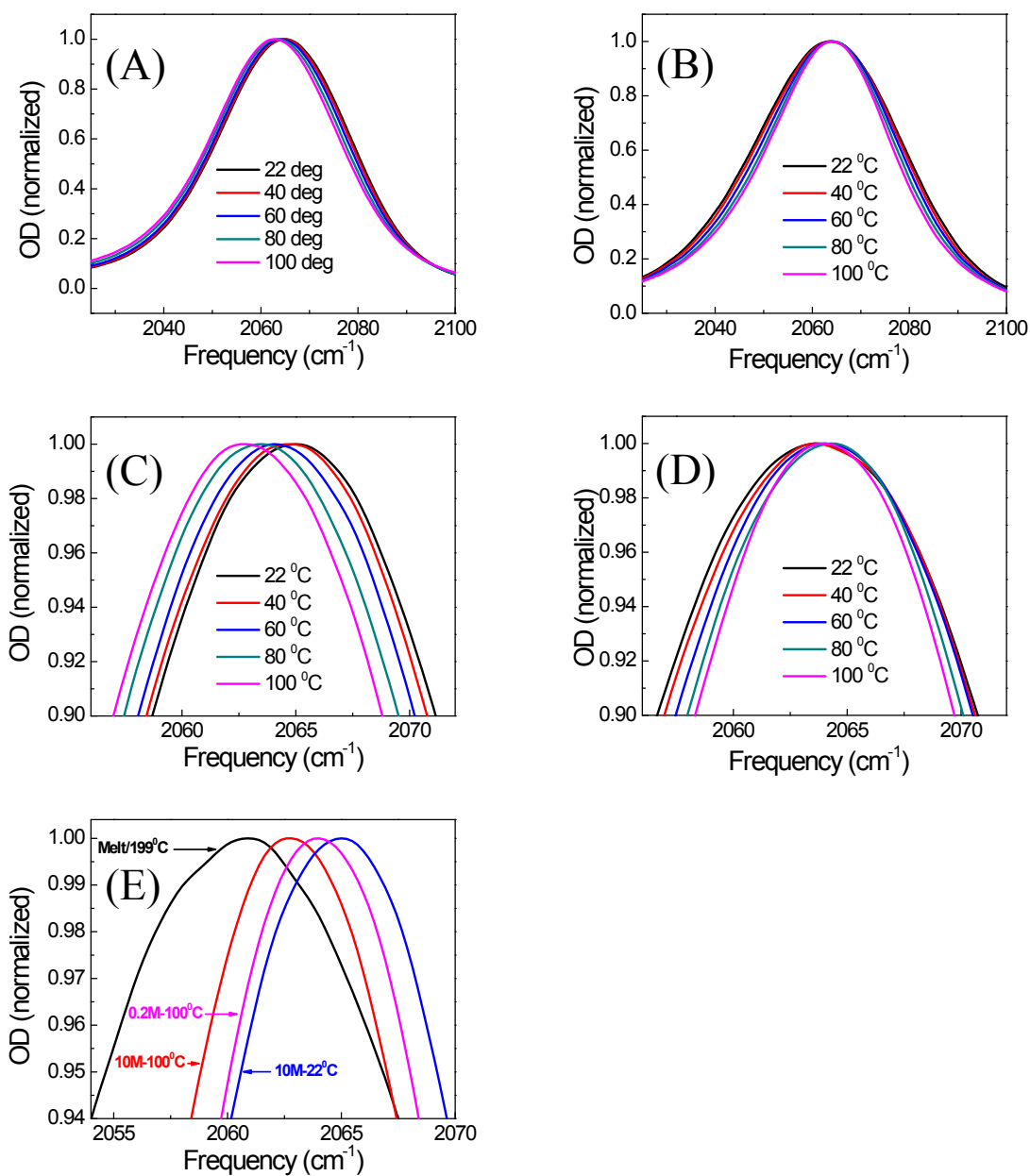


Figure S1. (A) Temperature dependent FTIR spectra of (A) 10M KSCN/D₂O solution, (B) 0.2M KSCN/D₂O solution, (C) enlarged part of (A), (D) enlarged part of (B), and (E) the KSCN melt (199°C, black) and KSCN 10M (100°C&22°C, red&blue) and 0.2M (100°C, magenta) solutions.

It is somewhat surprising that the CN 0-1 transition line width of the 10M KSCN

D₂O solution hardly changes with temperature. As shown in fig.S1A&C, the CN stretch peak line width remains constant from 22⁰C to 100⁰C and its peak position gradually redshifts for about 2.5 cm⁻¹. This is very different from those in the dilute 0.2M KSCN D₂O solution, as fig.S1B&D show that the line width becomes narrower at a higher temperature but the central frequency remains constant. A comparison among the CN stretch central frequencies in different environments (fig.S1E) show that the peak shift in the 10M solution from 22⁰C to 100⁰C passes by that of the dilute solution and goes closer to that of the KSCN melt (199⁰C). The observations suggest that at a higher temperature, KSCN ions in the concentrated aqueous solution tend to form more aggregates, which are probably similar to the melt rather than interact more with the water molecules. One possible reason is that at a higher temperature, the dielectric constant of water becomes smaller (from ~78 (RT) to ~56 (100⁰C)) and the SCN⁻/water interaction is weaker, as indicated with a narrower line width. A weaker solvent/solute interaction leading to a narrower vibrational line width was previously observed.^{1, 2} The FTIR results are consistent with the energy transfer measurements, as the kinetic analysis shows that at 80⁰C the ion cluster concentration in the 10M solution is 97% which is slightly larger than that (~95%) at room temperature and that the energy donor/acceptor distances are essentially the same at the two temperatures.

On the data analysis of KSCN/DMF solutions

Here we want to point out one issue. The ion cluster ratio estimated above is based on the fit of biexponential of which the two time constants can be adjusted within relatively large ranges. Such a treatment can cause relatively large uncertainties in ion cluster ratios, the number of anions inside one cluster, and the absolute values of energy transfer time constants. We found that the cluster ratio estimated in this way can vary from 40% to 60%, and the number of anion in one cluster can change from 7 to 3, and the resonant energy transfer time can vary from 30 to 80ps, and the one-donor/one-acceptor coupling strength can vary from 1.1 to 1.6 cm^{-1} . However, the ratio of the two nonresonant energy transfer time constants is independent of such a large uncertainty. It remains $\frac{k_{CN \rightarrow ^{13}C^{15}N}}{k_{CN \rightarrow ^{13}CN}} \cong \frac{1}{2}$. In other words, the predicted energy gap dependence of eq.5 holds for $\Delta\omega > 0$. This can be easily seen from the relative cross peak intensities at the same waiting times in the 2D IR spectra of KSCN/KS¹³C¹⁵N=1/1 and KSCN/KS¹³CN=1/1 solutions in fig.7B&E. The cross peak intensities of the KSCN/KS¹³CN=1/1 solution are about two times of those of the KSCN/KS¹³C¹⁵N=1/1 solution, indicating that the energy transfers between KSCN/KS¹³CN are about 100% faster than those between KSCN/KS¹³C¹⁵N.

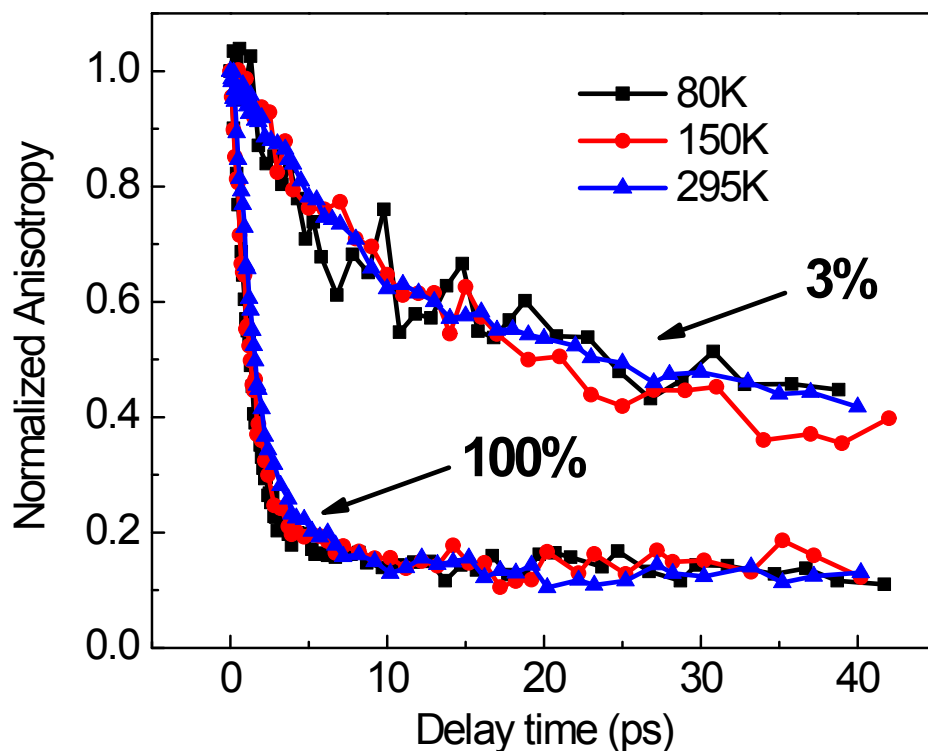


Figure S2. Temperature dependent anisotropy decays of the CN stretch (100% KSCN crystal) and the $^{13}\text{C}^{15}\text{N}$ stretch ($\text{KS}^{13}\text{C}^{15}\text{N}/\text{KSCN}=3/97$ mixed crystal) 1st excited state excitation signals. The curve of the pure KSCN crystal decays slightly faster at a lower temperature, indicating faster resonant energy transfers among the SCN⁻ anions. The simple single exponential fits to the data of 100% KSCN sample yield time constants at three temperatures: 1.32ps at 80K, 1.42ps at 150K, and 1.80ps at 295K.

The calculation parameters of the figures containing kinetic model calculations³

Fig. 6A&6B: The calculation parameters are

$$\begin{aligned}k_{SCN^-_{fast}} &= 1/3.6 (ps^{-1}); k_{SCN^-_{slow}} = 1/50 (ps^{-1}); \\k_{S^{13}C^{15}N^-_{fast}} &= 1/2.3 (ps^{-1}); k_{S^{13}C^{15}N^-_{slow}} = 1/51 (ps^{-1}); \\k_{SCN^- \rightarrow S^{13}C^{15}N^-} &= 1/95 (ps^{-1}); k_{S^{13}C^{15}N^- \rightarrow SCN^-} = 1/130 (ps^{-1}); \\A_{SCN^-_{fast}} &= 0.2; A_{S^{13}C^{15}N^-_{fast}} = 0.032; K = 30.\end{aligned}$$

Fig. 7C&7D: The calculation parameters are

$$\begin{aligned}k_{SCN^-_{fast}} &= 1/4.0 (ps^{-1}); k_{SCN^-_{slow}} = 1/50.0 (ps^{-1}); \\k_{S^{13}CN^-_{fast}} &= 1/5.0 (ps^{-1}); k_{S^{13}CN^-_{slow}} = 1/65.0 (ps^{-1}); \\k_{clu \rightarrow iso} &= 1/10 (ps^{-1}); k_{SCN^- \rightarrow S^{13}CN^-} = 1/570 (ps^{-1}); \\A_{SCN^-_{fast}} &= 0.14; A_{SCN^-_{slow}} = 0.86; \\A_{S^{13}CN^-_{fast}} &= 0.14; A_{S^{13}CN^-_{slow}} = 0.86; \\K &= 1.27; D=0.78; offset = 0\end{aligned}$$

Fig. 7F&7G: The calculation parameters are

$$\begin{aligned}k_{SCN^-_{fast}} &= 1/4.0 (ps^{-1}); k_{SCN^-_{slow}} = 1/55.0 (ps^{-1}); \\k_{S^{13}C^{15}N^-_{fast}} &= 1/5.0 (ps^{-1}); k_{S^{13}C^{15}N^-_{slow}} = 1/80.0 (ps^{-1}); \\k_{clu \rightarrow iso} &= 1/10 (ps^{-1}); k_{SCN^- \rightarrow S^{13}C^{15}N^-} = 1/1150 (ps^{-1}); \\A_{SCN^-_{fast}} &= 0.13; A_{SCN^-_{slow}} = 0.87; \\A_{S^{13}C^{15}N^-_{fast}} &= 0.06; A_{S^{13}C^{15}N^-_{slow}} = 0.94; \\K &= 1.27; D=0.70; offset = 0\end{aligned}$$

Fig. 8B&8C: The calculation parameters are

$$\begin{aligned}
k_{SCN^-_{fast}} &= 1/1.05 \text{ (ps}^{-1}\text{)}; k_{SCN^-_{slow}} = 1/589 \text{ (ps}^{-1}\text{)}; \\
k_{S^{13}CN^-_{fast}} &= 1/0.73 \text{ (ps}^{-1}\text{)}; k_{S^{13}CN^-_{slow}} = 1/688 \text{ (ps}^{-1}\text{)}; \\
k_{SCN^- \rightarrow S^{13}CN^-} &= 1/96 \text{ (ps}^{-1}\text{)}; k_{SCN^- \rightarrow S^{13}CN^-} = 1/123 \text{ (ps}^{-1}\text{)}; \\
A_{SCN^-_{fast}} &= 0.081; A_{S^{13}CN^-_{fast}} = 0.022;
\end{aligned}$$

Fig.8E&8F: The calculation parameters are

$$k_{CN} = k_{^{13}C^{15}N} = 1/545, k_{CN \rightarrow ^{13}C^{15}N} = 1/99 \text{ and } k_{^{13}C^{15}N \rightarrow CN} = 1/139.$$

Fig.10B&10C: The calculation parameters are

$$k_{CN} = 1/850, k_{^{13}C^{15}N} = 1/800, k_{CN \rightarrow ^{13}C^{15}N} = 1/163 \text{ and } k_{^{13}C^{15}N \rightarrow CN} = 1/333.$$

Fig.10E&10F: The calculation parameters are

$$k_{CN} = 1/1300, k_{^{13}C^{15}N} = 1/800, k_{CN \rightarrow ^{13}C^{15}N} = 1/237 \text{ and } k_{^{13}C^{15}N \rightarrow CN} = 1/912.$$

Fig.11B&11C: The calculation parameters are

$$k_{CN} = 1/1150, k_{^{13}CN} = 1/850, k_{CN \rightarrow ^{13}CN} = 1/296 \text{ and } k_{^{13}CN \rightarrow CN} = 1/477.$$

Fig.11E&11F: The calculation parameters are

$$k_{CN} = 1/1900, k_{^{13}CN} = 1/1400, k_{CN \rightarrow ^{13}CN} = 1/636 \text{ and } k_{^{13}CN \rightarrow CN} = 1/1590.$$

Fig.13B&13C: The calculation parameters are

$$\begin{aligned}
k_{SCN^-_{fast}} &= 1/150 \text{ (ps}^{-1}\text{)}; k_{SCN^-_{slow}} = 1/643 \text{ (ps}^{-1}\text{)}; \\
k_{S^{13}C^{15}N^-_{fast}} &= 1/147 \text{ (ps}^{-1}\text{)}; k_{S^{13}C^{15}N^-_{slow}} = 1/461 \text{ (ps}^{-1}\text{)}; \\
k_{SCN^- \rightarrow S^{13}C^{15}N^-} &= 1/68 \text{ (ps}^{-1}\text{)}; k_{S^{13}C^{15}N^- \rightarrow SCN^-} = 1/240 \text{ (ps}^{-1}\text{)}; \\
A_{SCN^-_{fast}} &= 0.01; A_{S^{13}C^{15}N^-_{fast}} = 0.01;
\end{aligned}$$

Fig.13E&13F: The calculation parameters are

$$\begin{aligned}
k_{SCN^-_{fast}} &= 1/0.62 \text{ (ps}^{-1}\text{)}; k_{SCN^-_{slow}} = 1/535 \text{ (ps}^{-1}\text{)}; \\
k_{S^{13}C^{15}N^-_{fast}} &= 1/5.31 \text{ (ps}^{-1}\text{)}; k_{S^{13}C^{15}N^-_{slow}} = 1/511 \text{ (ps}^{-1}\text{)}; \\
k_{SCN^- \rightarrow S^{13}C^{15}N^-} &= 1/162 \text{ (ps}^{-1}\text{)}; k_{S^{13}C^{15}N^- \rightarrow SCN^-} = 1/104 \text{ (ps}^{-1}\text{)}; \\
A_{SCN^-_{fast}} &= 0.19; A_{S^{13}C^{15}N^-_{fast}} = 0.10;
\end{aligned}$$

Original anisotropy data

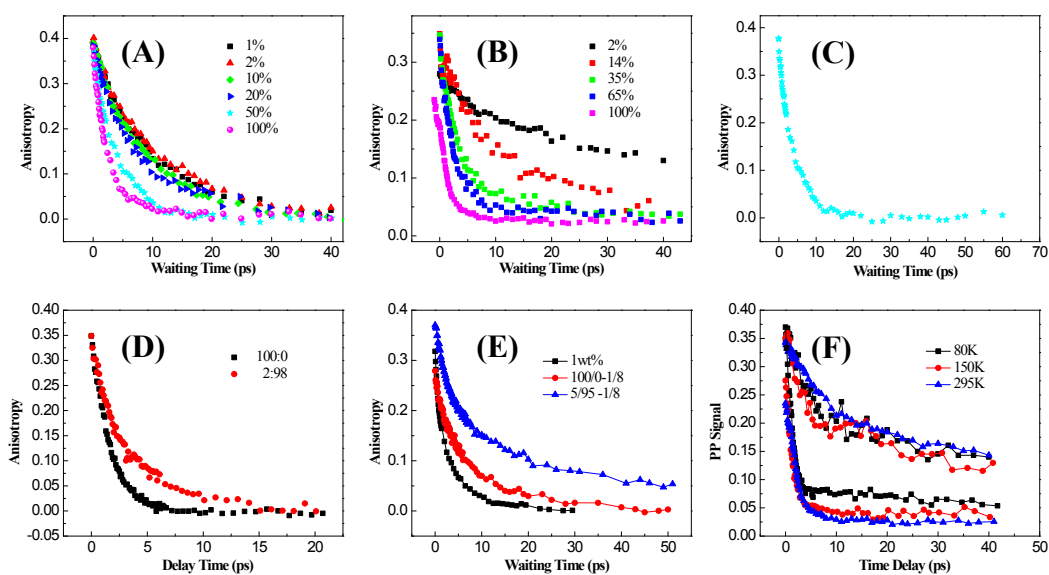


Figure S3. Original anisotropy data for (A) Fig. 2A, (B) Fig. 2B, (C) Fig. 4A, (D) Fig. 6C, (E) Fig. 7A and (F) Fig. S2. Because some of these data were not analyzed in the same time as the corresponding normalized anisotropy data, some curves may not be exactly the same as the ones after normalization. However, the conclusions are still not changed.

1. J. Zheng and M. D. Fayer, *J. Phys. Chem. B.*, 2008, **112**, 10221.
2. J. R. Zheng and M. D. Fayer, *J. Am. Chem. Soc.*, 2007, **129**, 4328-4335.
3. H. T. Bian, X. W. Wen, J. B. Li, H. L. Chen, S. Z. Han, X. Q. Sun, J. A. Song, W. Zhuang and J. R. Zheng, *Proc. Natl. Acad. Sci. U. S. A.*, 2011, **108**, 4737-4742.